PREPARATION AND CHARACTERIZATION OF PHASE-PURE ANATASE NANOPARTICLES

Dr Imad Ali Disher Al-Hydary
Department of Electrochemical Engineering
University of Babylon
Babil-Iraq
E-mail: imadali4@yahoo.com

ABSTRACT :-

The anatase phase of titania has great potential to be used in various applications. Thus; the synthesis of phase-pure nanocrystalline anatase has attained great importance in the past decade. In the present work, the sol-gel method was used to prepare such nanoparticles. It has been found that the sol-gel method can, with the help of long aging time, produce phase-pure anatase nanoparticles that have polygonal shape with edges' length in the range of (~30-70nm). The firing temperature should be kept higher than 500°C to get fully crystalline nanoparticles and lower than 800°C to avoid the phase transformation to rutile phase.

Keywords
Anatase, Rutile, Titania, Nanoparticles, Sol-gel method

الخلاصة :-

يمتلك طور الاناتيس لثنائي اوكسيد التيتانيوم الاهلية للاستخدامات العديدة في التطبيقات المختلفة، لذلك اكتسب تحضيره بشكل متبلور نانوي نقي–الطور اهمية كبيرة في العقد المنصرم. في العمل الحالي استعملت طريقة (المحلول–الجلاتين) في تحضير هذه المادة بالوصف المذكور. لقد وجد ان طريقة (المحلول–الجلاتين) يمكن ان تنتج هذه المادة بمساعدة التعتيق لفترة زمنية طويلة. تمتلك الحبيبات النانوية المحضرة شكلا متعدد الاظلاع تتراوح ابعاد اضلاعه بين (~30 – 70 نانومتر). يجب ان تتم عملية حرق الجلاتين في درجة حرارة اعلى من (500°م) للحصول على الحبيبات النانوية المتبلورة وبدرجة اقل من (800°م) لتفادي تكون طور الروتايل.

INTRODUCTION :-

Nanomaterials attractive interests due to their unusual properties, these properties are mainly belong to their high surface area to volume ratio. Based on these unusual properties, nanomaterials have the potential to be used in various applications **[Z. Guo 2009]**.
Among the nanomaterials, titanium dioxide got special interest because of its unusual optical, dielectrical, chemical, and catalytical properties. Accordingly, it has wide applications in various fields including photo catalysts, self cleaning materials, ultra white pigments, papers, cloth fibers, cosmetics, light scatterers, biocompatible materials and high refractive materials for optoelectronic devices **[H. K. Yu 2007]**.
Titania has three polymorphs, namely the anatase, brookite and rutile. The former two phases are the room-temperature phases and are transformed into the most stable rutile phase at higher temperature **[N. Jagtap 2005]**.
The anatase phase gets wide attention among the three polymorphs mentioned above. This is due to its great potential to be used for environmental purification, decomposition of carbonic acid gas, generation of hydrogen gas, and photocatalytic applications. Based on that, the synthesis of phase pure nanocrystalline anatase has attained great importance in the past decade. However, the presence of the rutile phase was a commonly noticed in many studies **[S. J. Limmer 2002, O. K. Varghese 2003, and D. Bhange 2006]**. Further, the stability of the anatase phase and the structural features of anatase titania have been the areas of strong research interest **[L. Jong 2003]**.
Titania nanomaterials have been synthesised by various techniques like chemical precipitation, anodization, electrodeposition, sol-gel, sonochemical deposition, and vapour deposition. Among these techniques, sol-gel technique offers many advantages, including low processing temperatures and high level of homogeneity **[O. K. Varghese 2003]**.
The aim of the current work is to prepare phase-pure anatase using sol-gel method making use of the ability of this method to produce a structure with molecular level homogeneity. This can help in producing phase-pure structure.

EXPERIMENTAL WORK :-

Titanium isopropoxide $Ti[OH(CH_3)_4]_4$ from Fluka (NLT 99%), ethanol from Qualigenes (NLT 99.5%), and acetone $(CH_3)_2CO$ from Qualigenes (NLT 99.5%) were used as such without further purification.
To prepare the sol, 6ml of titanium isopropoxide was dissolved in 40ml of ethanol at room temperature with magnetically stirring for 15min. The gel was prepared by adding 30ml of deionised water to the sol under stirring condition. After 10min of farther stirring, the gel was kept in the refrigerator at ~5°C for 10 days to complete the gelling process. The resulting gel was washed and separated using centrifugation technique. After overnight drying in oven at 100°C, the resulting powder was fired at 700°C for 3hrs with heating and cooling rate of 2°C/min.
Thermal gravimetric analysis (TGA) with simultaneous differential thermal analysis (SDTA) was performed on the powder in air with heating rate of 15°C/min from 25°C to 950°C using (Mettler-TG50). The as-synthesized powder was characterized for powder X-ray diffraction (Philips, Holland, X'Pert) using Ni-filtered $CuK\alpha_1$ over 2θ range from ~0° to 100°. Phase's identification was carried out by comparing the diffraction data with JCPDS standards. The morphology and size of prepared particles were studied from the micrograph of transmission electron microscope, TEM (Technai, Philips, Holland). The particles, after ultrasonically dispersion in ethanol for 15min, were deposited on a copper grid coated with carbon. Fourier transform infrared (FTIR) graphs were recorded of powder both before and after sintering using FTIR-8300 (Shimadzu, Japan) spectrometer. The specific surface area of the sintered

powder was determined by nitrogen adsorption analysis using Gemini-2375 (Micromeritics, USA) surface area and pore size analyzer by Brunauer, Emmett, and Teller (BET) method. Samples were degassed at 150°C for 2hr under vacuum before analysis.

RESULTS AND DISCUSSION

Figures **(1.A)** and **(1.B)** show the XRD patterns for the prepared particles before and after firing respectively. In both patterns, the obtained peaks are in full agreement with the corresponding values reported for anatase phase of titania (JCPDS, Card No. 21-1272). This indicates that the followed preparation method can produce crystalline phase before the firing process. This is an advantage comparing with the results of another work that produced amorphous material **[M. Kanna 2005]**. Comparing the relative intensities of both patterns shows that the peaks of the pattern (1.B) have sharpness higher than that of the peaks of the pattern (1.A). This indicates that the firing process, as expected, enhances the crystallinity of the particles. The broad peaks of the pattern (1.A) mark the presence of the nanoparticles. The patterns don't contain any peak neither for rutile phase (JCPDS, Card No. 21-1276) nor for brookite phase (JCPDS, Card No. 29-1360).

Crystallite sizes (S_{hkl}) were determined using Scherrer's formula **(1) [L. V. Azaroff 1968]**:

$$S_{hkl} = \frac{K\lambda}{\beta \cos\theta} \qquad (1)$$

where K is the shape coefficient with value between 0.9 and 1.0, λ is the X-ray wavelength, β is the full width at half maximum (FWHM) of each peak and θ is the diffraction angle. The estimated crystallite size along <200> and <004> planes were found to be 66nm and 32nm respectively.

Figures **(2.A)** and **(2.B)** show the FTIR spectra of the TiO_2 nanoparticles before and after firing respectively. The absorptions due to the vibration modes, which represent the anatase structure, have been noticed. Two bands assigned to Ti-O vibration have been noticed. The first at 500–800 cm^{-1} (broad peak) and the second at 1033cm^{-1}**[T. Busani 2005, K. Nakamoto 1986]**. These bands confirm the presence of TiO_2 phase in the prepared samples irrespective of sintering. For the non-fired samples, very broad bands were noticed assigned to water which has broad bands at 1630-1650 cm^{-1} and 3200-3350 cm^{-1}. After firing, these bands were reduced noticeably.

Figure **(3.A)** shows the TEM micrographs of the TiO_2 nanoparticles before firing. It can be seen that the sample was composed of highly agglomerated TiO_2 nanoparticles that have particles size less than 5 nm. The actual size and shape of these nanoparticles couldn't be identified even with very high magnification **(3.B)**. For this duty, high resolution transmission electron microscope is needed. After firing, these agglomerates converted to polygonal nanoparticles with different edges length in the range of (~30-70nm) as shown in figures **(3.C & 3.D)**. This result is well agreed with that of the XRD calculations.

Figures **(4.A)**, **(4.B)**, and **(4.C)** show the TGA, DTG, and SDTA graphs of the unfired nanoparticles. The TG curves show a remarkable weight loss up to 500°C. This loss can be seen, with the help of DTG curve, in two stages. The first stage represented by sharp weight loss, up to ~200°C, and the second stage is represented by subsequent gradual weight loss, up to 500°C. The initial weight loss is due to the dehydration of adsorbed water. The peak at 75-100°C in the DTG, which is attributed to liberation or decomposition of water molecules, supports this weight loss. The gradual weight loss, up to 500°C, is assigned to the crystallization of amorphous phase to anatase **[H. J. Youn 1999]** as the amorphous phases of

the TiO_2 always combine with Ti-OH bonds **[G. Sudant 2005]**. The total weight loss during the firing is found to be around 9% and it is mainly belong to removal of the water. The phase transformation from anatase to rutile starts at around ~800°C as shown in SDTA curve. This result is in agreement with that obtained by **[N. Jagtap 2005]** where the transformation started at around 750°C. This indicates that the prepared nanoparticles have high phase stability. Base on that the firing of the gel must be done between 500-800°C to get crystalline and phase pure anatase.

Figure **(5.A)** shows the plot of adsorption and desorption isotherms of the fired sample. This plot is matching with type II, which describe the adsorption by non porous solids **[S. J. Gregg 1982]**, of the six principal classes of isotherm shapes.

The average particle size in nm (*d*) was estimated based on equation (2) according to BET, Langmuir, and T-plot surface area for spherical particles (figures **5.B**, **5.C**, & **5.D**):

$$d = \frac{6}{\rho \cdot S_A} \qquad (2)$$

where S_A is the specific surface area in m^2/g, and ρ is the theoretical density in g/cm^3 **[T. Allen 1975]**.

Table **(1)** gives the values of the surface area and the corresponding estimated average particle size of the prepared nanoparticles. The estimated particle size according to BET, Langmuir, and T-plot surface area are in good agreement with the TEM observations. However, the same measurement showed that the sample has BJH pores surface area of $43m^2/g$. This indicates that Langmuir measurement gives more reasonable values of surface area for the sample because the total surface area of the powder can't be equal or less than the surface area of the pores created by their accumulation.

CONCLUSIONS :-

It has been found that the sol-gel method, with long aging time, is suitable for preparation of phase-pure anatase nanoparticles that have polygonal shape with edges' length in the range of (~30-70nm).

The firing of the dried gel should be achieved at temperature higher than 500°C, to get fully crystalline structure, and less than 800°C to avoid the phase transformation to rutile phase.

Langmuir measurement is most suitable, as compared with BET and T-plot surface area measurements, to measure the total surface area of the anatase nanoparticles.

Table (1) Values of the surface area and the estimated average particle size

Type of surface area	Surface area (m^2/g)	Estimated average particle size (nm)
BET	38	41
Langmuir	64	24
T-plot	44	36

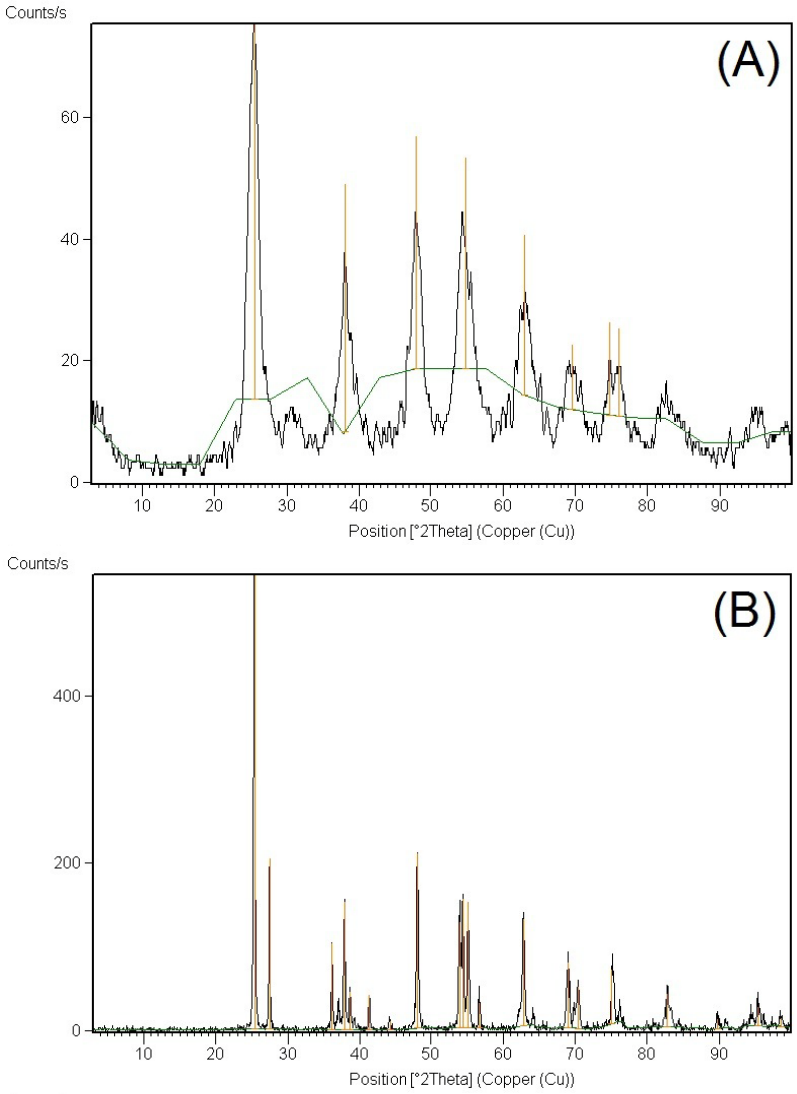

Figure 1.The XRD pattern of the prepared sample (A): before firing and (B) after firing

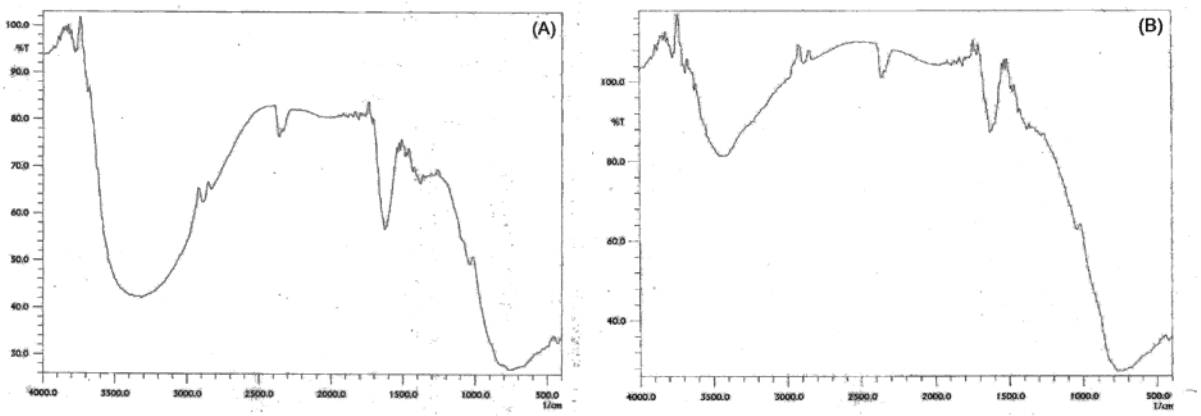

Figure 2.The FTIR spectra of the prepared sample (A): before firing and (B) after firing

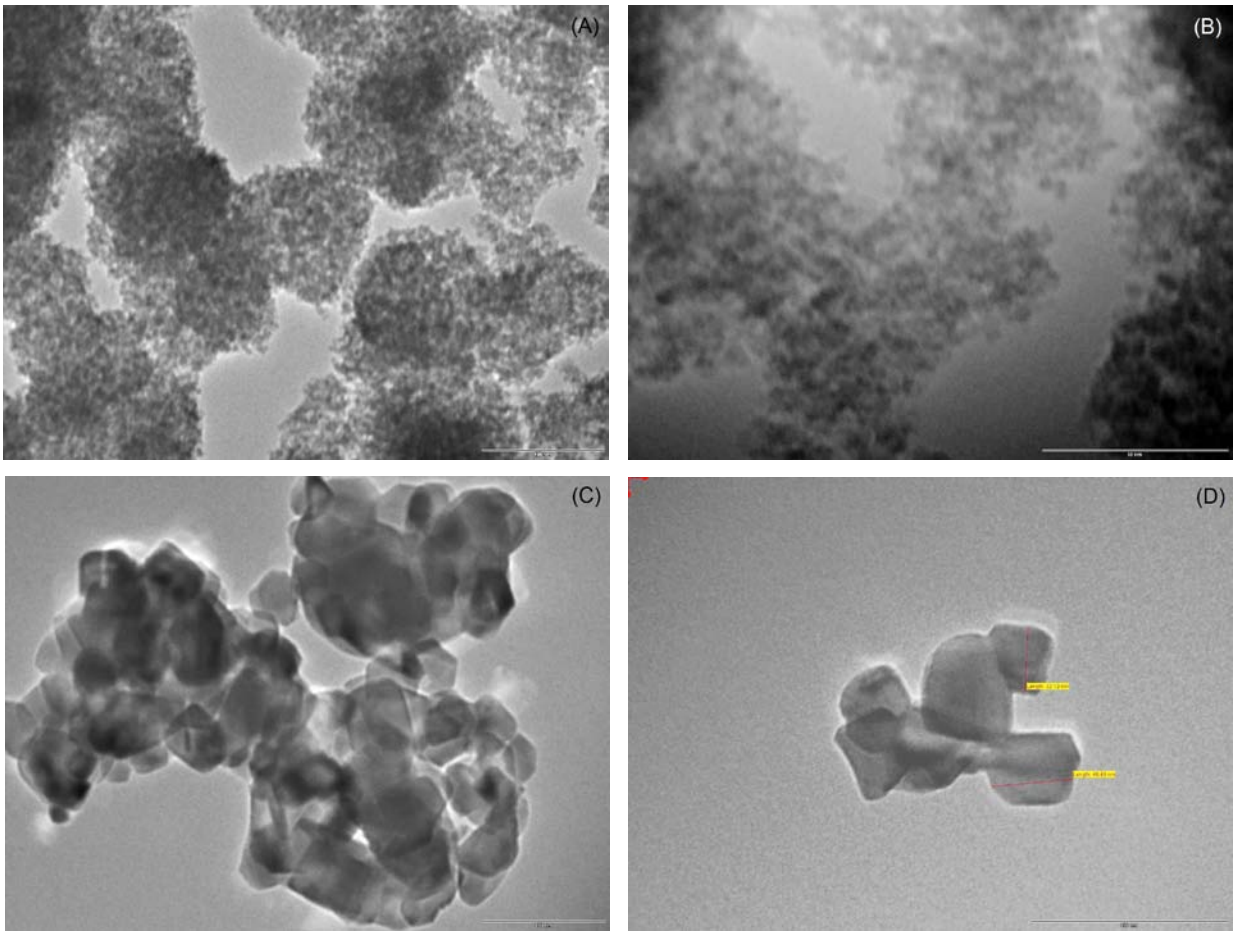

Figure 3.The TEM micrograph of the prepared sample (A & B): before firing, and (C & D) after firing (the scale bar length is 100nm in A, C, & D and 50nm in B)

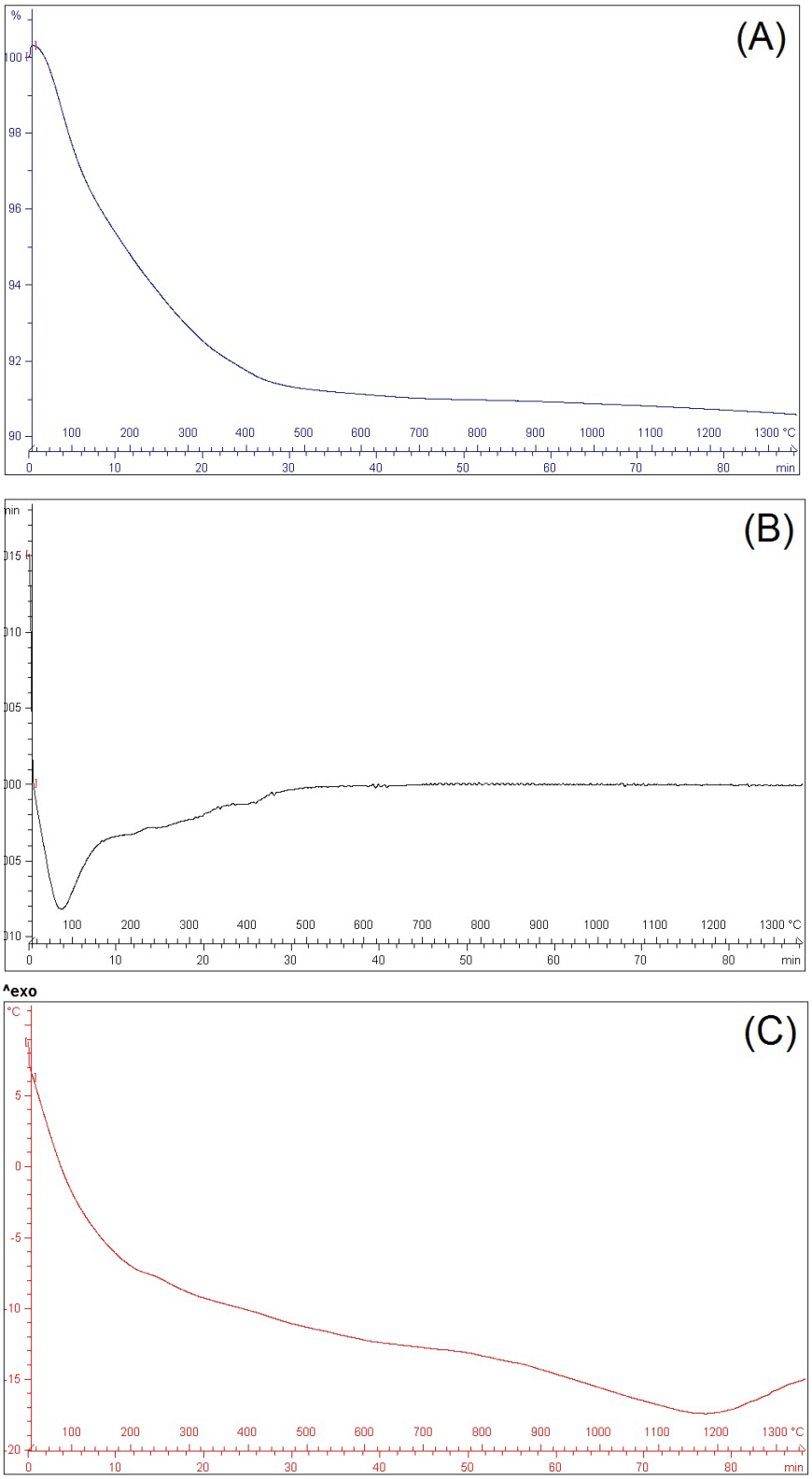

Figure 4.The thermal analysis diagrams of the prepared sample A: TGA, B: DTG, and C: SDTA

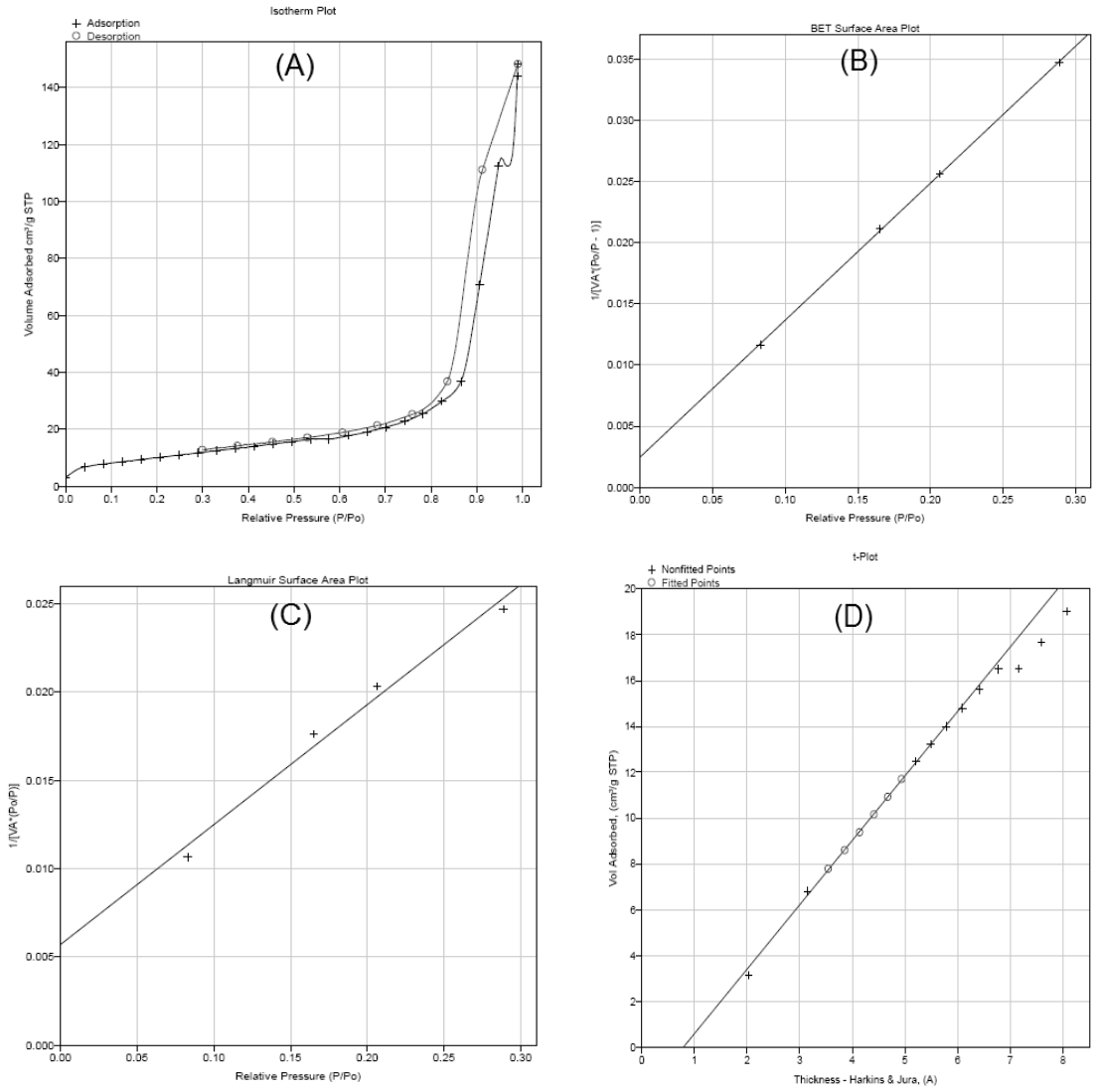

Figure 5.The surface area analysis of the prepared sample A: adsorption & desorption isotherm, B: BET surface area, C: Langmuir surface, and D: T-plot surface area

REFERENCES :-

D. Bhange and V. Ramaswamy, Synthesis of nanocrystalline titania by hydrothermal method using cetyl pyridinium chloride as a template and its catalytic applications, J. Cat. Com., 748, (2006)

G. Sudant, E. Baudrin, D. Larcher, and J. M. Tarascon, Electrochemical lithium reactivity with nanotextured anatase type TiO2, J. Mater. Chem.,15: pp1263-1269, (2005).

H. J. Youn, P. S. Ha, H. S. Jung, K. S. Hong, Y. H. Park, and K. H. Ko, Alcohol Rinsing and Crystallization Behavior of Precipitated Titanium Oxide, J. Colloid Interf. Sci., 211: pp 321-325, (1999).

H. K. Yu, T. H. Eun, G. R. Yi, and S. M. Yang, Multi faceted titanium glycolate and titania structures from room temperature polyol process, Journal of Colloid and Interface Science (316), 175–182, (2007)

K. Nakamoto, Infrared and Raman Spectra of Inorganic and Coordination Compounds, 4th edition, John Wiley & Sons, New York, p. 104, (1986).

L. Jong, H. N. Wooseok, K. Misook, H. G. Yong, Y. K. June, M. Ogino, K. M. Siezo, and C. S. Jin, Design of two types of fluidized photo reactors and their photocatalytic performances for degradation of methyl orange, Appl. Catal., A Gen. 244 (1), 49, (2003).

L. V. Azaroff, Elements of X-ray Crystallography, McGraw Hill Book Company, New York, (1968).

M. Kanna, S. Wongnawa, P. Sherdshoopongse, and P. Boonsin, Adsorption behavior of some metal ions on hydrated amorphous titanium dioxide surface, Songklanakarin J. Sci. Technol., 27(5) : 1017-1026, (2005)

N. Jagtap, Mahesh Bhagwat, Preeti Awati, and Veda Ramaswamy, Characterization of nanocrystalline anatase titania: an in situ HTXRD study, Thermochimica Acta (427), 37–41, (2005)

O. K. Varghese, D. Gong, M. Paulose, C. A. Grimes, and E. C. Dickey, Crystallization and high temperature structural stability of titanium oxide nanotube arrays, J. Mater. Res., Vol. 18, No. 1, (2003)

S. J. Gregg and K. S. W. Sing, Adsorption, Surface Area and Porosity, London: Academic Press, (1982).

S. J. Limmer, S. Seraji, Y. Wu, T. P. Chou, C. Nguyen, and G. Cao, Template-Based Growth of Various Oxide Nanorods by Sol-Gel Electrophoresis, Adv. Funct. Mater., 12, No. 1, (2002)

T. Allen, Particle Size Measurement, Chapman and Hall, (1975)

T. Busani, R. A. B. Devine, Dielectric and infrared properties of TiO2 films containing anatase and rutile, Semicond. Sci. Technol., 20: pp 870, (2005).

Z. Guo and L. Tan, Fundamentals and Applications of Nanomaterials, Artech House, (2009)